Poisonous Effects of Asteroid Impacts or Nuclear Explosions in the Western Regions of the Black Sea

Viorel Badescu*

Candida Oancea Institute, Polytechnic University of Bucharest, Bucharest, Romania

Received 11 September 2006; accepted 2 May 2007

ABSTRACT: The impact of an asteroid or a very large nuclear explosion in the Black Sea may cause a poisonous hydrogen sulfide gas release into the atmosphere. Some effects of this phenomenon on the western Black Sea coasts are evaluated in this paper. Two simple models are proposed to describe the generation of the H_2S cloud. The wind speed plays an important role in H_2S cloud dynamics. The land surface area covered by the H_2S cloud generated by a 1000-m-sized asteroid during the run-in ranges between about 4480 and 9600 km^2. This may affect up to 230 000 people. In the case of a 70-m-sized asteroid, the cloud covers between 70 and 210 km^2 of land. This may affect between about 1600 and 5100 people. The evaluations do not include the population of the towns on the seashore and may be a few times underestimated for some particular wind directions. These effects are briefly compared with more usual effects associated with asteroids impacting the sea, such as shock waves and tsunamis. Nuclear explosions of 1 and 50 Mton TNT may be assimilated to the impact by asteroids of about 33- and 120-m diameter, respectively.

KEYWORDS: Asteroid impact; Black Sea; Hydrogen sulfide; Impact phenomena; Anoxic and hypoxic environments; Biosphere/atmosphere interactions; Poisonous gas release; Down-wind dispersion

* Corresponding author address: Viorel Badescu, Candida Oancea Institute, Polytechnic University of Bucharest, Spl. Independentei 313, Bucharest 79590, Romania.
E-mail address: badescu@theta.termo.pub.ro

DOI: 10.1175/EI218.1

1. Introduction

The impact hazard from extraterrestrial bodies tends to evolve in the recent years from a pure scientific problem toward a serious societal issue. The environmental consequences from impacts are usually classified in three size ranges (Toon et al. 1997): (i) regional disasters due to impacts of multi-hundred-meter objects; (ii) civilization-ending impacts by multikilometer objects; and (iii) Cretaceous–Tertiary-like (K/T for short) cataclysms that yield mass extinctions. Recently, a number of researchers have argued that a fourth size range should be added, namely, (iv) multi-ten-meter impactors like Tunguska (Foschini 1999, and reference therein; Jewitt 2000).

The usual effects of asteroid impacts on water are atmospheric shock waves and tsunamis. An additional poisonous effect may be associated with impacts in the Black Sea, the largest anoxic water body on Earth. A scenario concerning the consequences of a not very large asteroid impacting the Black Sea was presented by us (Schuiling et al. 2005; Schuiling et al. 2007). In this paper we improve our previous model and a much more detailed analysis is performed. Two different mechanisms of hydrogen sulfide cloud formation are proposed. Different asteroid sizes are considered and various impact positions near the western coast of the Black Sea are taken into consideration. Estimates for the number of people living on or near the seashore that may be affected by the poisonous gas are performed. The effects of the poisoning gas on the population are briefly compared with the effects of shock waves and tsunamis. Consequences of nuclear explosions in the deep seawater of the Black Sea are briefly discussed at the end of the paper.

2. Information about the Black Sea

The Black Sea (Figure 1) is situated at 40°55′–46°32′N latitude, 27°27′–41°42′E longitude. It has a surface area of 422 000 km^2, a coastline length of 4090 km, and a maximum water depth of about 2200 m. About 87% of its volume below a surface layer of thickness 150–200 m is anoxic and therefore lifeless except for anaerobic bacteria. The Black Sea is Earth's biggest reservoir of hydrogen sulfide, which is generated by bacterial reduction of sulfate both in the water column and

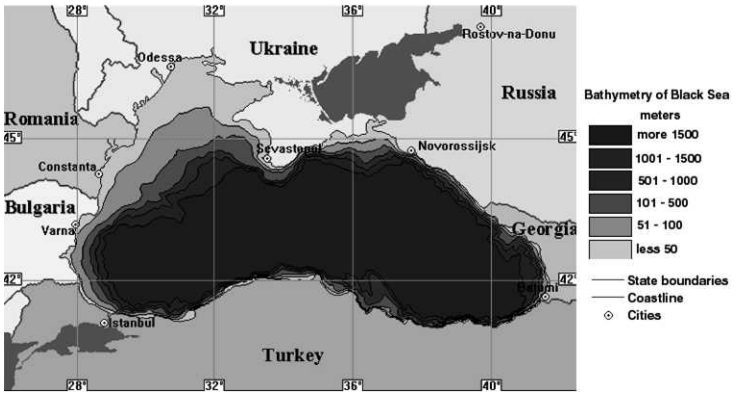

Figure 1. Geographical place and bathymetry of the Black Sea.

in the Holocene seafloor sediments (Schuiling et al. 2007). The surface layer is mostly generated by rain and freshwater inputs from rivers. Some authors believe that due to human interventions (dams on rivers; pollution of the seawater) this surface layer may become thinner in the future, resulting in H_2S bubbles entering the atmosphere (e.g., Humborg et al. 1997).

Both the salinity and the potential temperature increase with depth in the Black Sea waters. Data reported in Figure 1 of Neretin and Volkov (Neretin and Volkov 1999) are used in this paper. They refer to the seawater vertical temperature distribution measured on 7 November 1993 at station 4010 (43°30′N, 31°45′E; sea depth: 1910 m).

Studies of the hydrophysical and hydrochemical particularities of the deep water of the Black Sea are scarce due to the rather poor hydrophysical database. Data reported in Figure 3 of Neretin and Volkov (Neretin and Volkov 1995) are used in this paper. They refer to hydrogen sulfide vertical distribution measured on 9 August 1989 at station 4133 (43°20′N, 36°10′E; sea depth: 2163 m) and on 7 November 1993 at the above-mentioned station 4010.

3. Estimates of asteroid impact frequency in the Black Sea

A rough estimate for the impact frequency as a function of impactor size is given by Chapman et al. (Chapman et al. 2001): (i) multi-hundred-meter objects impact Earth every 10^4 yr, (ii) multikilometer objects impacts occur on a million-year time scale, and (iii) K/T-like cataclysms occur on a 100-Myr scale. Note that more recent results show a decrease by a factor of 4 in the estimated number of asteroids with diameter larger than 1 km (Ivezic et al. 2001).

Recent studies focused on the atmospheric penetration of small near-Earth asteroids. The asteroid composition proved to be very important. The models allow for energy loss by stony impactors below 200-m diameter, with complete disintegration (an airburst) below a diameter of about 100 m (Bland and Artemieva 2003). The results indicate that asteroids with a diameter greater than 200 m will hit the surface approximately once every 160 000 yr—way below previous estimates of impacts every 2500 yr. However, the number of impacts for iron asteroids of similar size was comparable with that predicted by older models.

A simple way to evaluate the frequency of asteroid impacts in the Black Sea is to multiply the estimations above (in years between successive collisions with similar sized objects) by the ratio between the Earth and Black Sea surface (which is 1208 for an Earth surface of 510 065 600 km^2) (Paine 1999).

4. Effects of asteroid impacts in the Black Sea

4.1. Phenomenology of asteroid impacts on the sea

Small impacting bodies may release their energy in the atmosphere. This depends, however, on the strength of the body. For example, both iron impacting bodies up to 20 m and comets as large as 200 m will deposit their energy in the atmosphere. Such air burst explosions are not efficient at delivering their energy to the ground. Here only impact bodies reaching the surface will be considered.

Very accurate numerical simulations provided valuable information about the interaction between larger-sized asteroids and the atmosphere, the seawater, and the underwater medium (Gisler et al. 2003). A brief review of these findings follows. Usually, less than 0.01 of the impactor's kinetic energy is dissipated during the atmospheric passage. The remaining part of the kinetic energy is absorbed by the ocean and seafloor within less than one second. The water immediately surrounding the impactor is vaporized, and the rapid expansion of the vapor excavates a cavity in the water. This cavity is asymmetric in case of oblique incidence angles, and the splash, or crown, is higher on the side opposite the incoming trajectory. The collapse of the crown creates a precursor tsunami that propagates outward. The higher part of the crown breaks up into droplets that fall back into the water. The hot vapor from the cavity expands into the atmosphere. When the vapor pressure diminishes enough, water begins to fill almost symmetrically the cavity from the bottom. The filling water converges on the center of the cavity and generates a jet that rises vertically in the atmosphere to a height comparable to the initial cavity diameter. It is the collapse of this central vertical jet that produces the principal tsunami.

Despite their accurate simulations, Gisler et al. (Gisler et al. 2003) concluded that an important question still remains to be answered, namely, how the kinetic energy of the impactor is partitioned among various processes, among which the volatiles' vaporization, the generation of a tsunami, and the cratering of the substrate are the most important.

4.2. Parametric model for asteroid impact on the Black Sea

A simple model will be developed to evaluate the effects of an asteroid impacting the Black Sea. The main assumption is that due to the collision, the asteroid's kinetic energy is entirely and almost instantaneously transformed into internal energy of both asteroid material and surrounding seawater. The entire asteroid material and some water around it vaporize explosively and are exhausted at high altitudes. Therefore, a cavity is generated into the seawater. This cavity constitutes "the source" for the subsequent phenomena. The liquid water displaced by the asteroid impact is fragmented during both the ascending and descending parts of its trajectory. This creates conditions for the gases dissolved in the water to be released into the atmosphere. Here we shall focus just on the hydrogen sulfide dissolved in the Black Sea waters.

Two different phenomena that may affect the coastal regions start simultaneously at the place of the asteroid impact. First, the initial water cavity constitutes the source for a tsunami wave. Second, the H_2S released into the atmosphere (which is denser than the air) finally creates a gaseous "cloud" or "blanket" on the sea surface. This H_2S cloud moves and disperses in the mean atmospheric wind field. The two phenomena have their own dynamics and their effects on the coastal regions are different.

4.2.1. The water cavity

The impact cavity in the sea is usually assimilated to a cylinder of radius R_c and depth D_c. The following general relationship between D_c and R_c is proposed by Ward and Asphaug (Ward and Asphaug 2000):

$$D_c = qR_c^{\alpha}, \tag{1}$$

where parameters q and α depend on asteroid properties. Only a fraction, ε_{cav}, of the asteroid's kinetic energy goes into making the cavity. The value of ε_{cav} is expected to range between 0.01 and 0.2 depending on various factors, among which the density of the impactor and the parameter q in Equation (1) are the most important. A value of $\varepsilon_{\text{cav}} = 0.03$ has been proposed in Paine (Paine 1999), but more recently we used $\varepsilon_{\text{cav}} = 0.15$ (Schuiling et al. 2007) as suggested by Kharif and Pelinovsky (Kharif and Pelinovsky 2005) and Kharif (C. Kharif 2005, personal communication). Hence the cavity depth is given by

$$D_c = \left(\frac{2\varepsilon_{\text{cav}}\rho_i R_i^3 V_i^2}{\rho_w g R_c^2}\right)^{1/2}, \tag{2}$$

where ρ_i, R_i, and V_i are asteroid density, radius, and velocity, respectively; and ρ_w is water density. Use of Equations (1) and (2) gives the diameter d_c of the cavity:

$$d_c \equiv 2R_c = 2R_i\left(\frac{2\varepsilon_{\text{cav}}V_i^2}{gR_i}\right)^{\delta}\left(\frac{\rho_i}{\rho_w}\right)^{\delta}\left(\frac{1}{qR_i^{\alpha-1}}\right)^{2\delta}, \tag{3}$$

with $\delta \equiv 1/[2(1 + \alpha)]$. One denotes by D_{eff} the thickness of the water layer displaced by the impact. Obviously

$$D_{\text{eff}} = \begin{cases} h_{\text{sea}} & (h_{\text{sea}} > D_c) \\ D_c & (h_{\text{sea}} \geq D_c) \end{cases}, \tag{4}$$

where h_{sea} is sea depth. The volume V_{eff} and the mass m_{sw} of this water layer are, respectively,

$$V_{\text{eff}} = D_{\text{eff}}\pi R_c^2 \quad m_{\text{sw}} = \rho_w V_{\text{eff}}. \tag{5), (6}$$

One denotes by f_{vap} that part of the seawater mass m_{sw} that is vaporized and explosively ejected at high altitudes. Accurate numerical experiments shows that f_{vap} is in the range from 0.05 to 0.2 (Gisler et al. 2003).

4.2.2. Tsunami generation

A model for tsunami generation and propagation due to an asteroid impacting the Black Sea was proposed by Schuiling et al. (Schuiling et al. 2007). Sample results are shown in the quoted work.

4.2.3. Hydrogen sulfide cloud generation

The mass of H_2S released in the atmosphere from the displaced water is

$$m_{H_2S} = k_{H_2S\uparrow}\rho_{H_2S,w}(1 - f_{\text{vap}})V_{\text{eff}}, \tag{7}$$

where $\rho_{H_2S,w}$ is the average H_2S concentration in the seawater and $k_{H_2S\uparrow}$ is a coefficient (valued between 0 and 1) showing how much H_2S is released in the atmosphere from the ejected seawater.

The H_2S released will mix with the atmospheric air. The H_2S–air mixture will form a blanket (cloud) over the sea surface. The mass participation of H_2S in the

mixture is denoted by g_{H_2S}. Here, g_{H_2S} is valued between 1 (for a pure H_2S blanket) and near 0 (for very small quantities of H_2S in the air).

It is reasonable to assume that the blanket is a cylinder of radius R_c. The thickness of the blanket h_{mixture} may be computed from

$$h_{\text{mixture}} = \frac{V_{\text{mixture}}}{\pi R_c^2}, \tag{8}$$

where V_{mixture} is blanket volume, which may be computed from the ideal gas state equation:

$$pV_{\text{mixture}} = m_{\text{mixture}} R_{\text{mixture}} T_{\text{mixture}}. \tag{9}$$

Here the mixture pressure p equals (in first approximation) the ambient (undisturbed) atmospheric pressure. The mass m_{mixture} of the air–H_2S mixture in Equation (9) is given by

$$m_{\text{mixture}} = \frac{m_{H_2S}}{g_{H_2S}}, \tag{10}$$

while the mixture constant R_{mixture} is computed by

$$R_{\text{mixture}} = \frac{R_M}{M_{\text{mixture}}}, \tag{11}$$

where R_M ($\cong$8314 J kmol^{-1} K^{-1}) is ideal gas constant and M_{mixture} is the mixture molar mass given by

$$\frac{1}{M_{\text{mixture}}} = \frac{g_{H_2S}}{M_{H_2S}} + \frac{1 - g_{H_2S}}{M_{\text{air}}}, \tag{12}$$

where M_{H_2S}($\cong$34 kg kmol^{-1}) and M_{air}($\cong$28.9 kg kmol^{-1}) are H_2S and air molar masses, respectively.

Results obtained from the energy balance show that the average water temperature in the impact area is just a few degrees higher than the initial seawater temperature in case of impactors with a 70–300-m diameter. When impactors of 1100-m diameter are considered, the water temperature increases by as much as 30°C. It seems reasonable to assume that the H_2S–air mixture temperature T_{mixture} in Equation (9) equals the averaged (on depth) seawater temperature T_w, taking into account that the H_2S was released from that deep seawater and the large value of the water heat capacity.

The dynamics of the hydrogen sulfide release in the atmosphere and the formation of the H_2S cloud are very complex processes. Therefore, the evaluation of the parameters $k_{H_2S\uparrow}$ and g_{H_2S} is not a simple problem. Two models based on different mechanisms of hydrogen sulfide release will be used here to provide a rough solution. In the following they are referred to as model A and model B. A combination of these (and other) mechanisms would arise in reality.

Model A assumes that most of the hydrogen sulfide is released from the liquid seawater ejected at high altitude by asteroid explosion during its fall as fragments

of different sizes. The mass transfer surface is very large and Henry's law may be tentatively used:

$$p_{H_2S,air} = k_H \rho_{H_2S,w}, \tag{13}$$

where $p_{H_2S,air}$ is the released H_2S partial pressure in the atmosphere and k_H (= 11.5 atm L mol^{-1}) is Henry's constant for hydrogen sulfide dissolved in water at 20°C (ATSDR 1999). The averaged (on sea depth) hydrogen sulfide density is $\rho_{H_2S,w} \approx 8$ g m^{-3}. From Equation (13) one finds the partial pressure of H_2S in the mixture, $p_{H_2S,air} \approx 0.0027$ atm. Use of the ideal gas equation for normal pressure and temperature gives the hydrogen sulfide density in the mixture $\rho_{H_2S,air} \approx 3.96$ g m^{-3}. The hydrogen sulfide release process is spread over the whole region with falling water. Therefore, a reasonable assumption is that the volume of the H_2S cloud is comparable with that of the falling water, which in turn is almost equal to the volume of the initial water cavity. This gives the ratio $\rho_{H_2S,air}/\rho_{H_2S,w} \approx 0.5$ as an estimate for the parameter $k_{H_2S\uparrow}$. The volumetric participation of hydrogen sulfide in the mixture is $r_{H_2S} = p_{H_2S,air}/(p + p_{H_2S,air}) \approx 0.002\ 69$. Use of the standard formula $g_{H_2S} = r_{H_2S}M_{H_2S}/[r_{H_2S}M_{H_2S} + (1 - r_{H_2S})M_{air}]$ yields the mass participation of H_2S in the mixture: $g_{H_2S} \equiv 0.0031$. Several hypotheses were implicit in the above simple model. First, chemical equilibrium was assumed when Henry's law was used. In fact, the duration of water falling is finite and chemical equilibrium is probably not reached. This assumption leads to overestimated values of $k_{H_2S\uparrow}$. Second, normal pressure and temperature values (i.e., 0.101 325 MPa and 273.15 K, respectively) were assumed throughout the hydrogen sulfide cloud. In fact, this cloud may be many hundreds of meters in height and the average pressure in the cloud is of course lower than the normal pressure. This assumption leads to underestimated values of g_{H_2S}. Third, with hydrogen sulfide release the chemical equilibrium is changed and Henry's law should normally be used again with other entries for the density of the H_2S dissolved in water. To take account of these simplifications the covering values $k_{H_2S\uparrow} = 0.4$ and $g_{H_2S} = 0.003$ will be used in calculations.

Model B assumes that most of the hydrogen sulfide is released from the falling liquid seawater when it is splashed by collision with the sea surface. In this case the hydrogen sulfide release is a more violent surface process. One expects the release degree to be higher and the H_2S cloud thickness to be much smaller than in case of model A. In computations we shall use $k_{H_2S\uparrow} = 0.7$ and we shall assume the extreme case when the cloud consists of pure hydrogen sulfide ($g_{H_2S} = 1$). This scenario was already used by Schuiling et al. (Schuiling et al. 2007).

5. Basic information about hydrogen sulfide

5.1. Hydrogen sulfide in nature

A brief review of the most important properties of hydrogen sulfide follows (Chou 2003). At room temperature H_2S is a colorless, flammable gas with a characteristic odor of rotten eggs. Its vapor pressure is 1929 Pa (at 21.9°C). Hydrogen sulfide is soluble in water, alcohol, ether, glycerol, gasoline, kerosene, crude oil, and carbon disulfide. Its water solubility is 1 g in 242 mL (at 20°C). The taste threshold for hydrogen sulfide in water is between 0.05 and 0.1 mg L^{-1}

(WHO 1993). Hydrogen sulfide may evaporate easily from water. In general, low pH and high temperature tend to favor evaporation (HSDB 1998). The conversion factor for hydrogen sulfide in air (20°C, 101.3 kPa) is 1 mg m^{-3} = 0.71 ppm. Other physical and chemical properties of hydrogen sulfide can be found in the International Chemical Safety Card (IPCS 2000).

Releases to the environment are primarily in emissions to the atmosphere, where it usually remains for less than 1 day, but in winter may persist for as long as 42 days. Hydrogen sulfide in the air is oxidized by molecular oxygen and hydroxyl radicals, forming the sulfhydryl radical and ultimately sulfur dioxide or sulfate compounds (Hill 1973; Thompson 1976). Sulfur dioxide and sulfates are eventually removed from the atmosphere through precipitation or absorption by plants and soils.

5.2. Effects of hydrogen sulfide on humans

Most data about the effects of hydrogen sulfide on humans are derived from acute poisoning case reports, occupational exposures, and limited community studies. Reported health effects in humans following exposure to hydrogen sulfide include death and respiratory, ocular, neurological, cardiovascular, metabolic, and reproductive effects. The geometric mean odor threshold for a large population is 11 μg m^{-3}. At concentrations greater than 140 mg m^{-3}, olfactory paralysis occurs. A few breaths at 700 mg m^{-3} can be fatal. There are many case reports of human deaths after single exposures (i.e., exposure to a chemical for up to 24 h) to high concentrations (larger than 700 mg m^{-3}) of hydrogen sulfide gas (Beauchamp et al. 1984). Most of them have occurred in relatively confined spaces; the victims lost consciousness quickly after inhalation of hydrogen sulfide, sometimes after only one or two breaths (the so-called "slaughterhouse sledgehammer" effect). Table 2 of Chou (Chou 2003) gives quantitative results about human health effects at various hydrogen sulfide concentrations.

6. Dynamics of hydrogen sulfide clouds

For low-momentum dense gas releases at ground level on uniform, level terrain with unobstructed atmospheric flow, the buoyancy-dominated, stably stratified, and passive dispersion regimes can be modeled with the Dense Gas Dispersion (DEGADIS) model (Havens and Spicer 1985; Havens 1988a; Havens 1988b). A few details about this model follow (Spicer and Havens 1992). If the primary source (gas) release rate exceeds the maximum atmospheric take-up rate, a denser-than-air gas blanket is formed over the primary source. This near-field, buoyancy-dominated regime is modeled using a lumped parameter model of a denser-than-air gas "secondary source" cloud, which incorporates air entrainment at the gravity-spreading front using a frontal entrainment velocity. If the primary source release rate does not exceed the maximum atmospheric take-up rate, the released gas is taken up directly by the atmosphere and dispersed downwind. For either source condition, the downwind dispersion phase of the calculation assumes a power law concentration distribution in the vertical direction and a modified Gaussian profile in the horizontal direction with a power law specification for the wind profile. The source model represents a spatially averaged concentration of gas present over the

primary source, while the downwind dispersion phase of the calculation models an ensemble average of the concentration downwind of the source. The ambient wind field is characterized by a known velocity u_0 at a given height z_0, a surface roughness z_R, and the Pasquill stability class.

The DEGADIS model does not take the hydrogen sulfide oxidation rates into account. Thus, the next results represent "worst case" calculations in this respect. Recent experimental and simulation studies of volcanic plumes show that the atmospheric reactions for H_2S strongly depend on the halogens' existence (Aiuppa et al. 2006). The results suggest that models not including the chemistry of H_2S in the atmosphere may give reasonably accurate information in case halogens are missing from the poisonous gas cloud.

7. Model implementation

Various scenarios concerning asteroid impact were considered. The Bulgarian and Romanian seashores were envisaged in this paper as possible regions to be affected. This western Black Sea coast has a rather dense population, which strongly increases during summer, as a result of tourism.

7.1. Population distribution

The most recent Gridded Population of the World (GPW2) dataset (CIESIN 2006) provides information about the spatial distribution of population. Figure 2 shows the spatial distribution of population in countries on the western coast of the Black Sea. The most populated cities on the seashore are Varna (43.20°N, 27.55°E, with 314 539 people in 1996) and Burgas (42.50°N, 27.47°E, with 199 470 people in 1996) in Bulgaria; and Constanta (44.18°N, 28.65°E, with 346 830 people in 1997) and Mangalia (43.50°N, 28.35°E, with 44 271 people in 1992) in Romania. Except for the large cities and for some inhabited regions of the Danube Delta, the population density near the seashore ranges between 5 and 249 persons per square kilometer.

7.2. Asteroid size and properties

Several asteroid sizes will be considered. A Tunguska-sized asteroid ($D_i = 70$ m) is one of our choices. It belongs to size class iv (see section 1). Two other size class ii asteroids are also analyzed: they have diameters of 250 and 1000 m. The asteroid material is assumed to be either dunite (mass density 3200 kg m^{-3}) as a mockup for typical stony asteroids or steel (7800 kg m^{-3}) as a mockup for nickel–iron asteroids (Gisler et al. 2003). Some values adopted here for various quantities are shown in Table 1.

7.3. Asteroid impact location

Before starting a more detailed analysis, asteroid impacts were simulated over the whole Black Sea surface. The radius and depth of the generated water cavity was evaluated. For any potential impact position, the content of dissolved hydrogen sulfide in the waters was estimated by using the following simple procedure. The distance between an impact position and the two locations with available

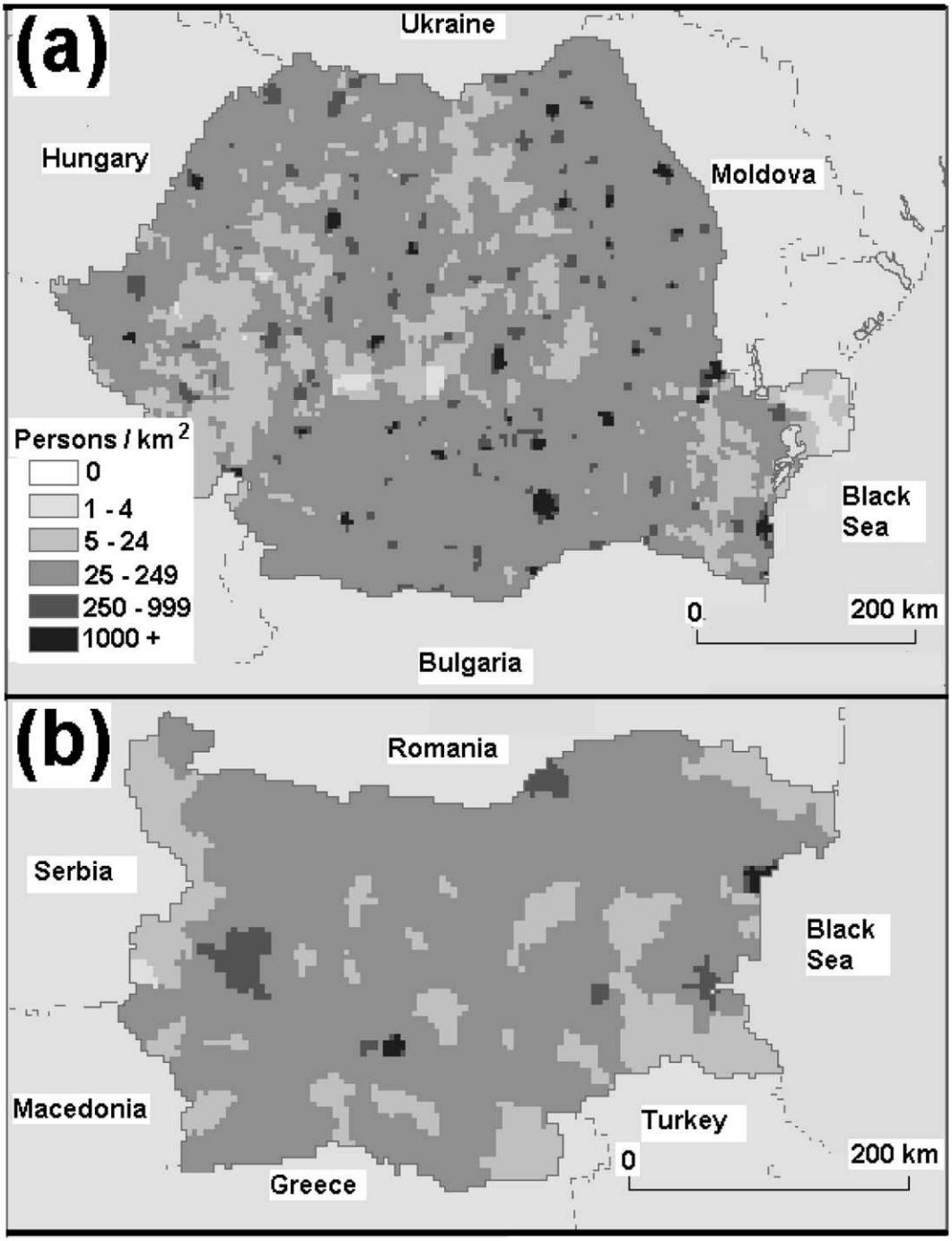

Figure 2. Population distribution on the western coast of the Black Sea: (a) Romania and (b) Bulgaria. (Source: CIESIN 2006).

Table 1. Values adopted in calculations.

Quantity	Symbol	Value
Asteroid (impactor)		
Density (kg m^{-3})	ρ_i	3200 (for $D_i = 250$ m and 1000 m) 7800 (for $D_i = 70$ m)
Velocity (m s^{-1})	V_i	20 000
Impact parameters		
Parameter entering Equation (1)	α	1.27
Parameter entering Equation (1)	q	0.1
Parameter entering Equation (2)	ε	0.15
H_2S cloud		
H_2S release fraction	$k_{H_2S\uparrow}$	0.4 (model A) 0.7 (model B)
H_2S participation in the cloud	g_{H_2S}	0.003 (model A) 1 (model B)

experimental data [i.e., station 4133 and station 4010, respectively, in Neretin and Volkov (Neretin and Volkov 1995)] was computed and the measured vertical distribution of hydrogen sulfide content from the nearest location was adopted. The distribution was truncated, or linearly extrapolated, to take into account the difference between the seawater depth at the impact location and at the measurement stations, respectively. Accurate bathymetry data for the Black Sea (Smith and Sandwell 1997) were used in calculations. An average value of the H_2S content over the water column was finally computed. The hydrogen sulfide cloud parameters (i.e., thickness and diameter) were determined for all potential impact positions. Both models A and B described in section 4.2.3. were considered.

Figure 3 shows as an example the thickness of the hydrogen sulfide cloud generated by an asteroid of size $D_i = 250$ m impacting all of the Black Sea. Model A was considered. The cloud thickness may be as large as 1200 m. It is obvious that the cloud thickness is larger in case where the asteroid is impacting deeper waters (cf. the lines of equal seawater depth in Figure 1 and the lines of equal cloud thickness in Figure 3, respectively). The white area outside the dashed isoline shows that generation of hydrogen sulfide clouds is not possible because the water depth is less that 200 m. Note that when model B is considered, the maximum pure H_2S cloud thickness is a few meters (see Table 2).

Three asteroid impact positions were considered in a more detailed study. They are denoted as 1 (43.12°N, 28.9°E; sea depth: −1229 m), 2 (43.12°N, 29.4°E; sea depth: −1723 m), and 3 (43.12°N, 29.9°E; sea depth: −1634 m). These locations are about 40 km away from each other. A fourth impact location, denoted as 0 (43.12°N, 28.62°E; sea depth: −134 m), will be considered during the analysis. This location is placed in the area where no hydrogen sulfide cloud is generated. All these locations were selected to have the same latitude as Varna (Figure 4).

7.4. Wind data

The interaction of the poisoning gas cloud with the population on the coast depends strongly on the direction and speed of the wind. Measured wind speed and wind direction data for the Black Sea may be found in the SeaWinds database (see http://www.ssmi.com/qscat/qscat_description.html). Statistical analysis of

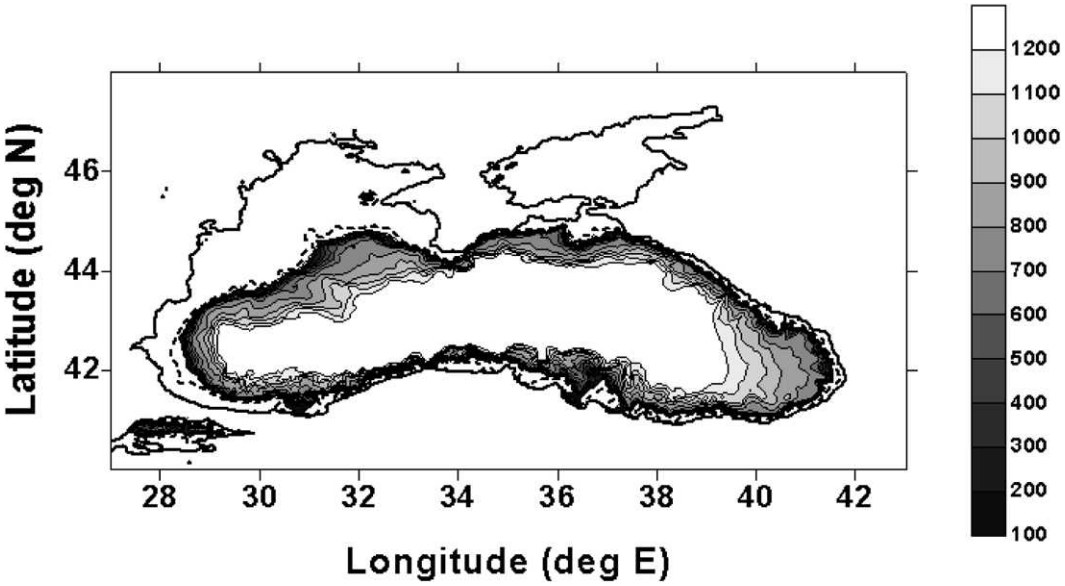

Figure 3. Thickness (m) of a hydrogen sulfide cloud generated by potential impacts of a 250-m-diameter asteroid all over the Black Sea surface. Model A of cloud generation was considered. No cloud is generated outside the dashed line.

SeaWinds data shows that the wind direction near the western coast of the Black Sea changes with time (Figure 5). Of particular interest for our study are the time periods with wind direction toward the land. We found such periods during April, June, July, and October. The wind speed and direction are, of course, random in

Table 2. Initial cloud thickness and initial mass of the hydrogen sulfide in the cloud as a function of asteroid diameter, impact location (see Figure 4), and the model adopted for cloud formation (i.e., model A or model B).

Asteroid diameter (m)	Model of cloud formation	Impact location	Cloud thickness (m)	Hydrogen sulfide mass (Gg)
70	A	1–3	513	8.2
	B	1–3	1.91	14.4
250	A	1	722	42.0
		2	891	51.9
		3	844	49.1
	B	1	2.69	73.5
		2	3.32	90.8
		3	3.15	86.0
1000	A	1	722	262.5
		2	891	324.0
		3	844	307.0
	B	1	2.60	262.5
		2	3.32	567.0
		3	3.15	537.0

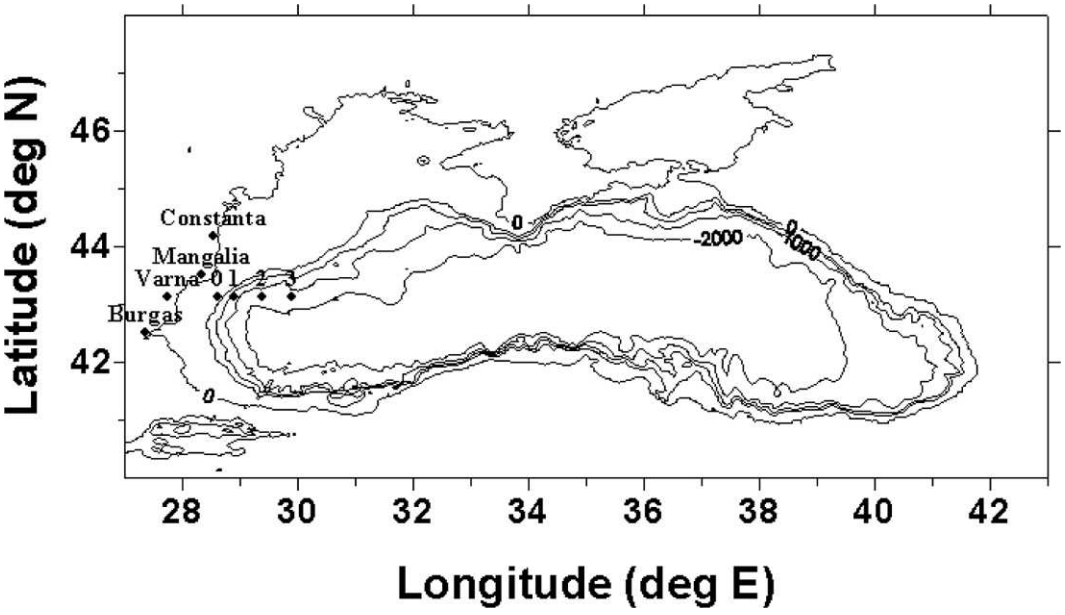

Figure 4. Asteroid impact positions (0, 1, 2, and 3) and major cities on the western coast of the Black Sea.

nature. Some correlation between wind speed and direction on 10 and 11 April 2003 is shown as an example in Figure 6. The following convention was adopted: winds blowing toward the north are denoted by 0° (or 360°) and winds blowing toward the east are denoted by −90°. The predominant wind direction is about −235° and the wind speed may be as high as 10 m s^{-1}. Figure 6 shows that the wind statistics may keep a rather similar pattern for two consecutive days. There is a tendency for the wind speed to increase during the autumn when it may be as high as 16 m s^{-1}.

8. Results and discussions

Computations were made for downwind dispersion of the cloud consisting of hydrogen sulfide, air, and water vapor.

No hydrogen sulfide cloud is generated at impact position 0, because the seawater depth is small and does not contain dissolved hydrogen sulfide. At the other impact positions, the initial ($t = 0$) diameter of the hydrogen sulfide cloud depends on asteroid size. It is about 2580, 4916, and 12 288 m, for $D_i = 70$, 250, and 1000 m, respectively, whatever the impact location is. One expects that the initial ($t = 0$) thickness of the cloud depends, in addition, on sea depth at impact location and on the model adopted for cloud formation (i.e., A or B). Model B estimates a larger H_2S mass in the cloud than model A does, whatever the asteroid size (Table 2). Larger clouds are generated by larger-sized asteroids, as expected. Also, both the cloud thickness and the H_2S mass it contains are larger at impact positions with deeper seawater. However, for small-sized asteroids ($D_i = 70$ m) cloud thickness

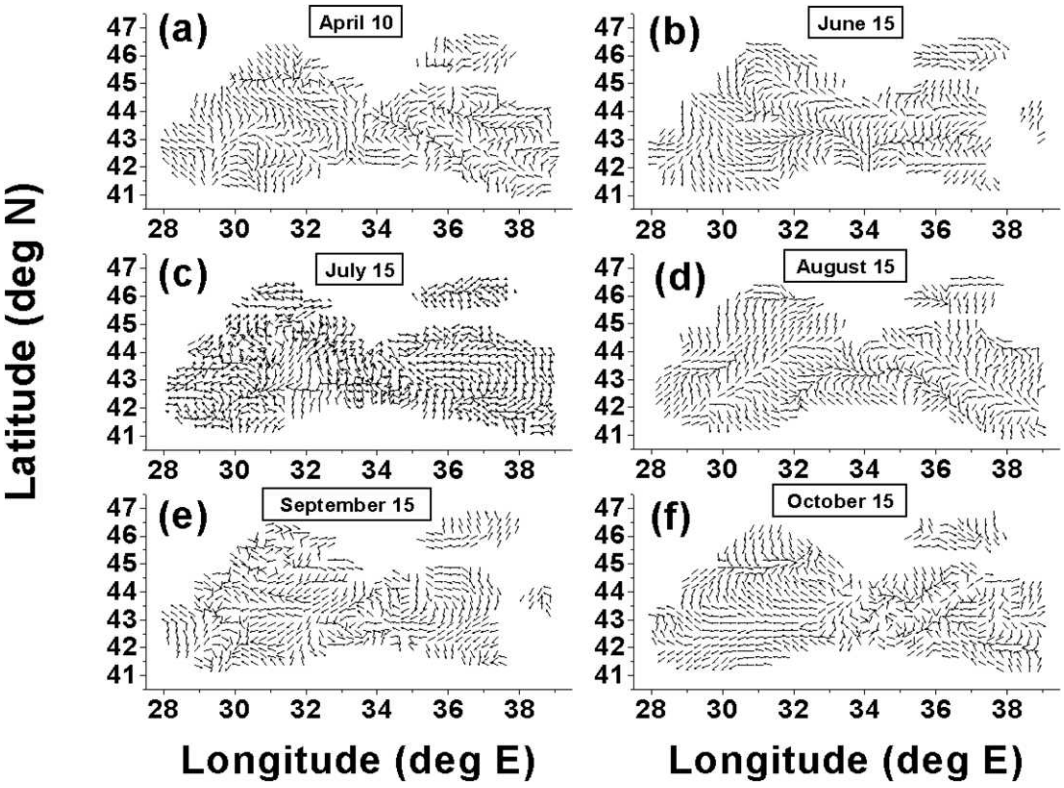

Figure 5. Daily averaged wind directions over the Black Sea for various days in 2003: (a) 10 Apr, (b) 15 Jun, (c) 15 Jul, (d) 15 Aug, (e) 15 Sep, and (f) 15 Oct.

does not depend on impact position. This is explained by the fact that the depth of the water cavity ($D_c = 892$ m) created by the impact is smaller than the sea depth for all the three impact locations.

The distance between the asteroid impact location and a given location on the seashore was evaluated by two analytical procedures, that is, by considering the orthodrome and loxodrome path, respectively. These procedures are useful when the geographical coordinates of both locations are known. A third combined analytical–numerical procedure was also used to find the distance between the impact location (described by its latitude and longitude) and the closest location on land for a given (loxodrome) direction. This procedure uses the accurate Black Sea bathymetry data given by Smith and Sandwell (Smith and Sandwell 1997). The estimates by the three procedures, though close to each other, do not coincide. This may be explained by principal differences but also by the fact that the geographical coordinates of large towns are not associated with locations placed precisely on the seashore. Table 3 gives the distance between the impact locations and the main localities on the western coast of the Black Sea evaluated by the combined analytical–numerical procedure.

In the analysis reported below two values are considered when referring to hydrogen sulfide concentrations: the lower concentration limit (LLC) of 19.88

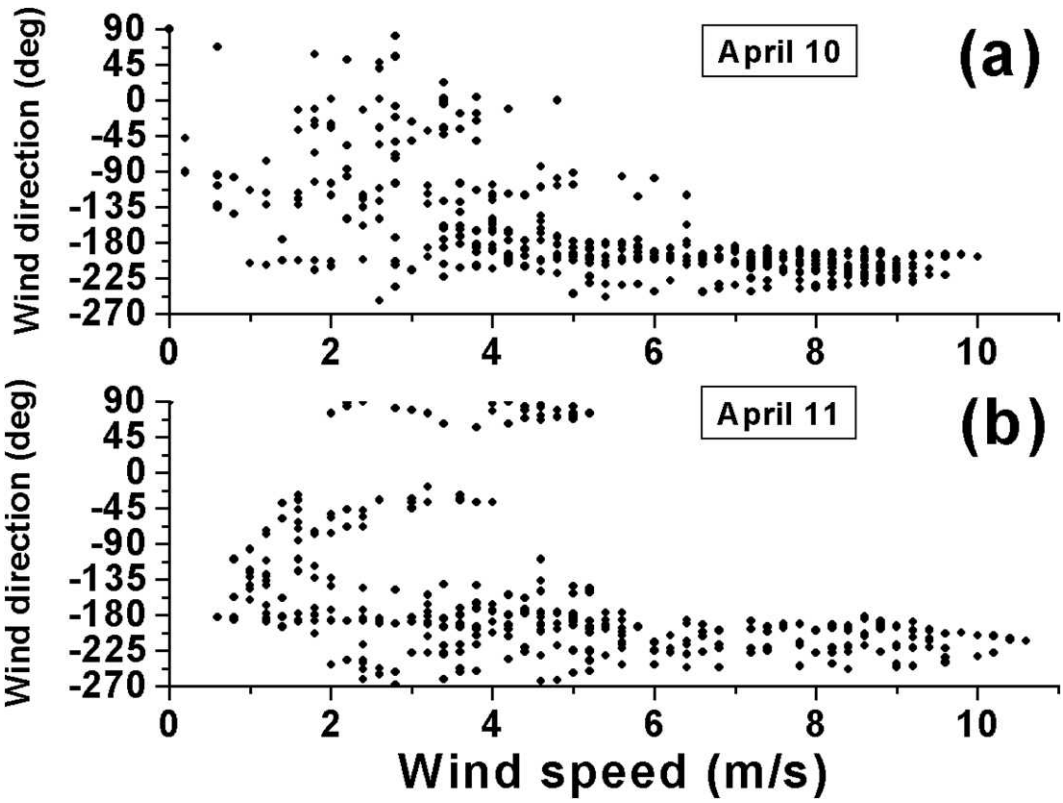

Figure 6. Daily averaged wind direction vs daily averaged wind speed on (a) 10 Apr 2003 and (b) 11 Apr 2003. Winds blowing toward the north: 0°. Winds blowing toward the east: −90°.

ppm and the upper concentration limit (ULC) of 497 ppm. These values are associated with the following effects on humans. The LLC corresponds to fatigue, loss of appetite, headache, irritability, poor memory, and dizziness (Ahlborg 1951). The ULC corresponds to death after single exposure (Beauchamp et al. 1984). The lowest concentration of interest (i.e., LLC = 19.88 ppm) is the concentration at which the calculations by the DEGADIS model are stopped.

The dynamics of the hydrogen sulfide cloud generated at the three impact locations was simulated by using the DEGADIS model. Different sizes of asteroids

Table 3. Distance (km) between the asteroid impact locations and some localities on the western coast of the Black Sea (see Figure 4). The smallest distance for a given impact position is shown in bold.

Impact location	Varna	Burgas	Mangalia	Constanta
0	71	123	**48**	118
1	93	142	**61**	121
2	134	179	**95**	136
3	174	217	**132**	160

were considered. Both A and B models for poisonous cloud generation were envisaged. Two wind speeds are adopted in most of the following calculations, namely $u_0 = 5$ m s^{-1} and $u_0 = 10$ m s^{-1}, respectively, both of them at $z_0 = 10$ m height. They may be considered as rather common values and should not be seen as extremes.

The amount of turbulence in the atmosphere is very often categorized by the Pasquill stability classes A, B, C, D, E, and F. Class A denotes the most turbulent conditions and class F denotes the least turbulent conditions, which are usually associated with nighttime and a total cloud cover amount less than 50%. Class D applies to heavily overcast skies, at any wind speed, day or night, while class C applies to days with strong incoming solar radiation and rather low wind speed (Beychok 2005). The adopted stability Pasquill class needed by the DEGADIS model is F. During the first simulations three wind directions were considered. A zonal wind was first assumed (i.e., its direction is parallel to the latitude and oriented toward the west). The other two directions differ by +30° and −30°, respectively, from the first direction. Other wind directions were considered during the analysis.

It is interesting to see the dynamics of the hydrogen sulfide cloud at a very low wind speed. This will give a perspective for the more realistic simulations reported below. Figure 7 shows the status at various moments of the H_2S cloud generated by an asteroid of diameter $D_i = 250$ m at impact position 1. The wind speed is $u_0 = 0.5$ m s^{-1} and model B of the cloud formation was adopted. All results refer to the elevation of 2 m above sea level. The width from the cloud centerline to the indicated concentration levels at the indicated height is shown in the cases of the LLC and ULC, respectively. Figure 7a shows that even a long time after the impact ($t = 70\,600$ s) the cloud is almost centered on the impact location, denoted by 0 in the abscissa. The asymmetry induced by wind direction is, however, obvious. Note that the cloud dimensions, both parallel and perpendicular on wind direction, are comparable in size. The ULC cloud core is smaller and more sensitive to wind speed than the LLC cloud core, as expected. Figure 7b shows the last moment when the DEGADIS model emphasizes the existence of the ULC core in the cloud (note that the adopted time step is 7000 s in this particular case). This ULC core lasted for more than 33 h and it traveled in wind directions less than 40 km from the impact location. However, it did not reach the land (see Table 3 for distances to various localities at the seashore). Note that the DEGADIS model accounts for the complex downwind dispersion process and the "traveled" distance by the cloud margins is of course larger than the distance evaluated by the usual formula (wind speed × time period). Figure 7c shows the last moment when the DEGADIS model shows the existence of the LLC core in the cloud. This core lasted for about three days and it traveled on wind directions about 75 km. It may reach Mangalia if the wind direction is constantly oriented for three days toward this town.

Figure 8 shows sample results for simulations with the same input data as those of Figure 7, except for the wind speed, whose value is $u_0 = 10$ m s^{-1} this time. A short time after the impact, the asymmetry induced by wind direction is already obvious and the two cloud dimensions (i.e., parallel and perpendicular on wind direction) are comparable in size (Figure 8a). Also, the ULC cloud core is comparable in size to the LLC core. The nearest locality to impact position 1 is Mangalia (see Table 3). Thus, the most dangerous wind direction is toward this

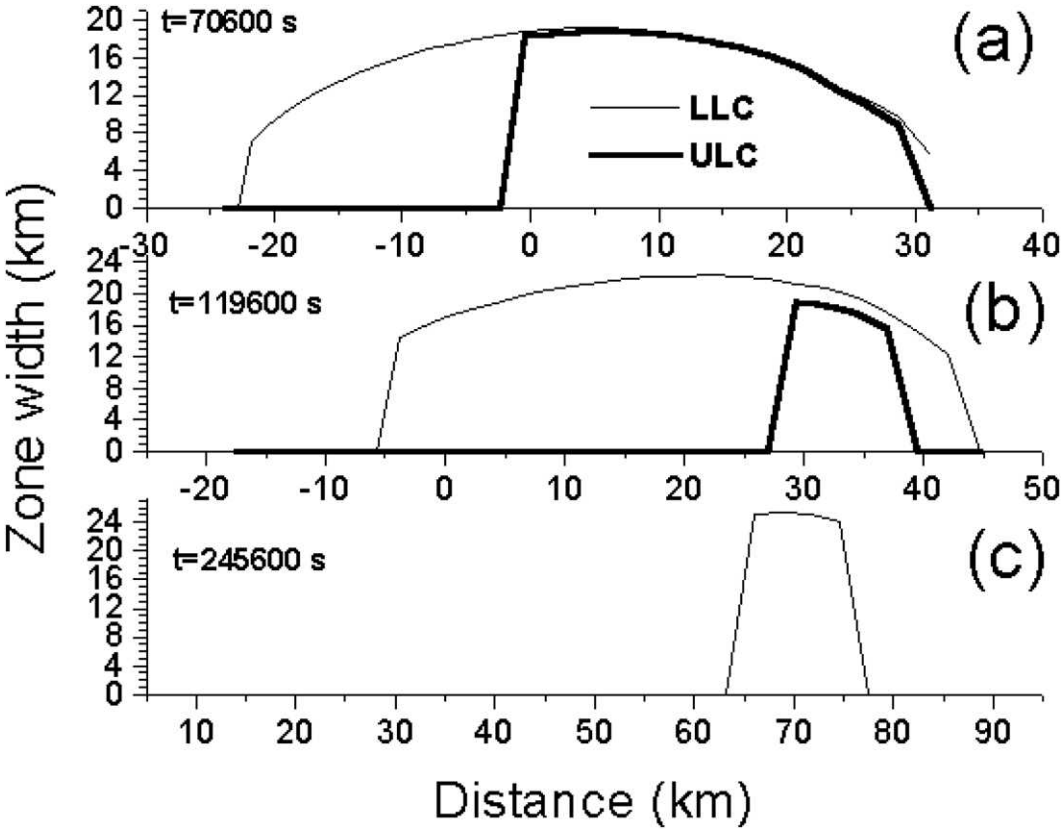

Figure 7. Time and space dependence of the ULC and LLC core width from the cloud centerline, respectively: (a) 70 600, (b) 119 600, and (c) 245 600 s after asteroid impact. All data refer to the elevation of 2 m above sea level. ULC denotes the H_2S upper limit concentration; LLC denotes the H_2S lower limit concentration. The distance is measured downwind from the impact location. A 250-m-diameter impactor was considered. The wind speed is 0.5 m s^{-1}.

town. This case is considered next. Figure 8b refers to a time moment when H_2S concentrations higher than ULC just arrived over the coast of Mangalia. This happens about 1 h and 20 min after the impact. The cloud is more diluted as reported in Figure 8a. This is shown by the rather important difference between the widths of the ULC core and LLC core. The LLC zone width from the cloud centerline is about 2 km larger than the corresponding ULC zone width. The cloud "length" in wind direction is about 15 km while its maximum length perpendicular to wind direction is of the order of 10 km. Figure 8c shows the last moment when the DEGADIS model shows the existence of the ULC core in the cloud. This core, with a size of about 4 km × 10 km, entered the land by more than 10 km in about 17 min. By using the terminology used in the tsunami research area, one may call the travel of the hydrogen sulfide cloud over the land the "run-in." During its run-in, the ULC cloud core covered about 100 km^2 of land. Figure 2a shows that the population density around Mangalia is about 25 to 249 people per square

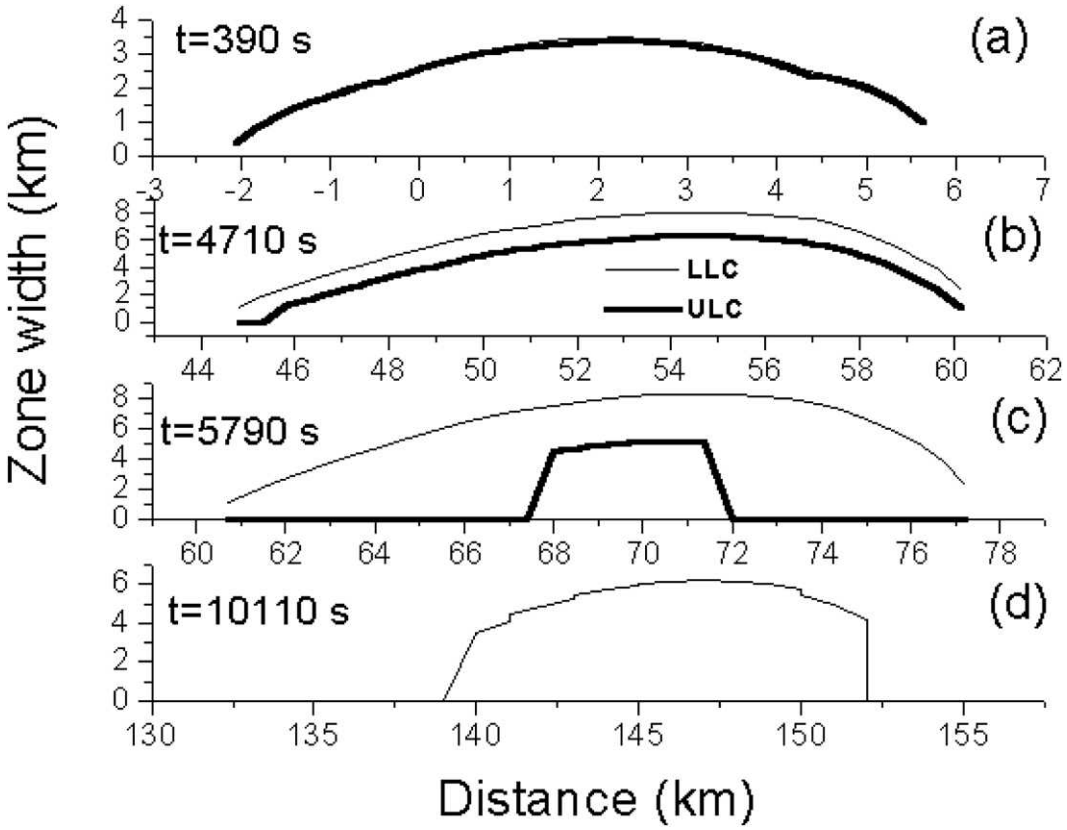

Figure 8. Same as in Figure 7, but for (a) 390, (b) 4710, (c) 5790, and (d) 10 110 s after asteroid impact. The wind speed is 10 m s^{-1}.

kilometer. Thus, the population affected by the ULC cloud core may be as large as 2500 to 24 900 people (apart from Mangalia's habitants). Figure 8d shows the last moment when the DEGADIS model shows the existence of the LLC core in the cloud. This core entered the land by about 90 km in about 1.5 h. Its last size is about 12 km × 12 km. The LLC cloud core covered about 1080 km^2 during its run-in and the number of people affected may be as large as 27 000 to 268 000.

The maximum distance traveled by the ULC cloud core increases significantly by increasing the asteroid size, as expected (Figure 9). Also, this distance increases by increasing the wind speed. Generally, the influence of the impact position on the distance traveled by hydrogen sulfide clouds is weak, whatever the asteroid diameter is. This is explained by the fact that seawater is rather comparable in depth at all three impact positions.

In the case of 1000-m-diameter asteroids, both models A and B predict comparable distances traveled by the ULC cloud core. They are about 120 and 140 km at 5 and 10 m s^{-1} wind speed, respectively. Note that doubling the wind speed is associated with a rather small increase in the traveled distance by the cloud. This shows the important contribution of the diffusion in the complex downwind process modeled by the DEGADIS model. The values of the traveled distance by the

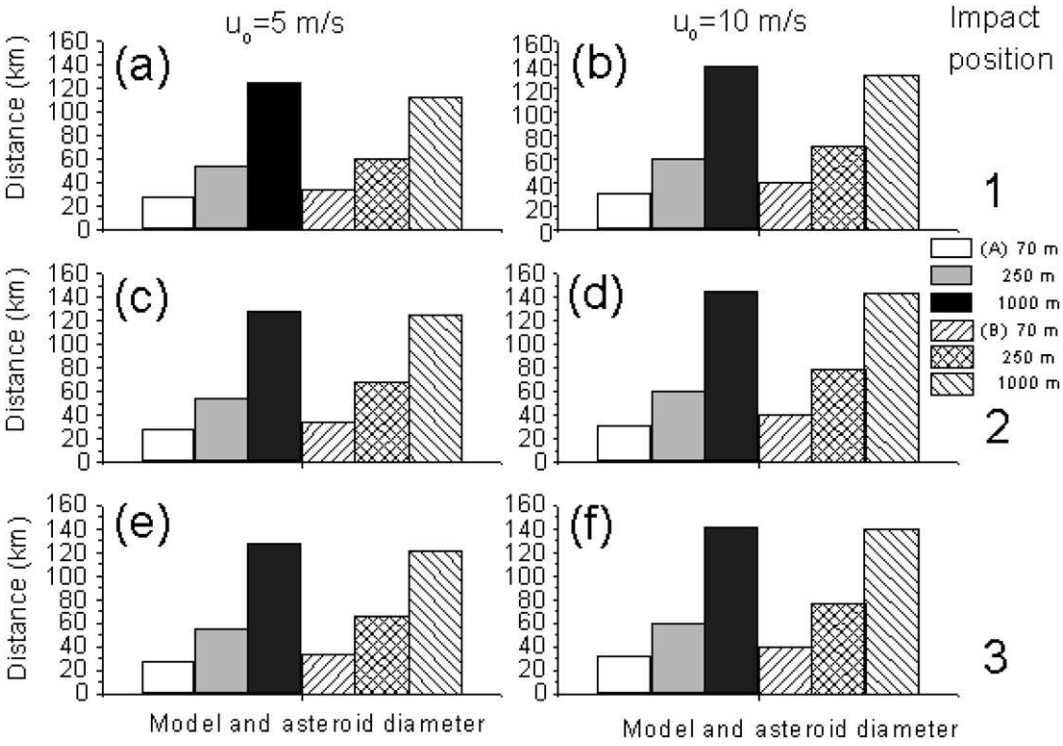

Figure 9. Maximum distance traveled by the ULC cloud core as a function of impact location, asteroid diameter, wind speed, and model adopted to describe hydrogen sulfide cloud generation. (a) Impact position 1, wind speed u_0 = 5 m s^{-1}; (b) impact position 1, wind speed u_0 = 10 m s^{-1}; (c) impact position 2, wind speed u_0 = 5 m s^{-1}; (d) impact position 2, wind speed u_0 = 10 m s^{-1}; (e) impact position 3, wind speed u_0 = 5 m s^{-1}; and (f) impact position 3, wind speed u_0 = 10 m s^{-1}. ULC denotes the H_2S upper limit concentration. All data refer to the elevation of 2 m above sea level. The distance is measured downwind from the impact location.

cloud may be compared with distances in Table 3. Mangalia is particularly accessible for clouds generated at all three impact positions. Varna and Constanta are exposed to clouds generated at impact position 1 (wind speed of about 5 m s^{-1}) and to a lesser extent to clouds generated at impact position 2 (wind speed of about 10 m s^{-1}). Burgas is accessible to clouds generated at impact position 1 but only for wind speeds greater than 10 m s^{-1}. Impacts at position 3 do not affect Burgas, Constanta, or Varna. The run-in of ULC cloud core may range between 0 and about 80 km, depending on wind speed and direction. Computations show that the size of the ULC cloud core is about 24 km perpendicular to wind direction. The land surface area covered by the ULC cloud core during the run-in may be as high as 1920 km^2. The population density on some regions of the Bulgarian seashore ranges between 5 and 24 persons per square kilometer. On the remaining Bulgarian seashore and the Romanian coast it ranges between 25 and 249 persons per square kilometer. One estimates that the ULC cloud core may affect between about 9600

and 478 000 people, depending on wind direction (apart from the population of the large towns on the shore).

Model B estimates larger distances than model A does when smaller-sized asteroids (i.e., 70 and 250 m) are considered. The ULC cloud cores generated by 70-m-diameter asteroids travel for about 30 km and do not reach the shore, whatever the impact position is. When 250-m asteroids are considered, the ULC cloud core travels between 60 and 75 km, depending on model and wind speed. Mangalia is the only town that may be reached by this ULC cloud core if an asteroid impacts position 1 with the appropriate wind direction. An estimate of the population affected by the ULC cloud core generated by 250-m asteroids was already presented in connection with Figure 8c.

The maximum distance traveled by the LLC cloud core increases significantly by increasing the asteroid size, as expected (Figure 10). Also, this distance increases by increasing the wind speed but does not significantly depend on the impact position. Generally, model B estimates shorter distances traveled by the LLC cloud core than model A does, whatever the impactor size and wind speed are.

In the case of 1000-m-diameter asteroids, the distances traveled by the LLC cloud core range between about 260 and 290 km (depending on model) at a wind speed of 5 m s^{-1} and between about 300 and 360 km (depending on model) at a wind speed of 10 m s^{-1}. These values may be compared with distances in Table 3.

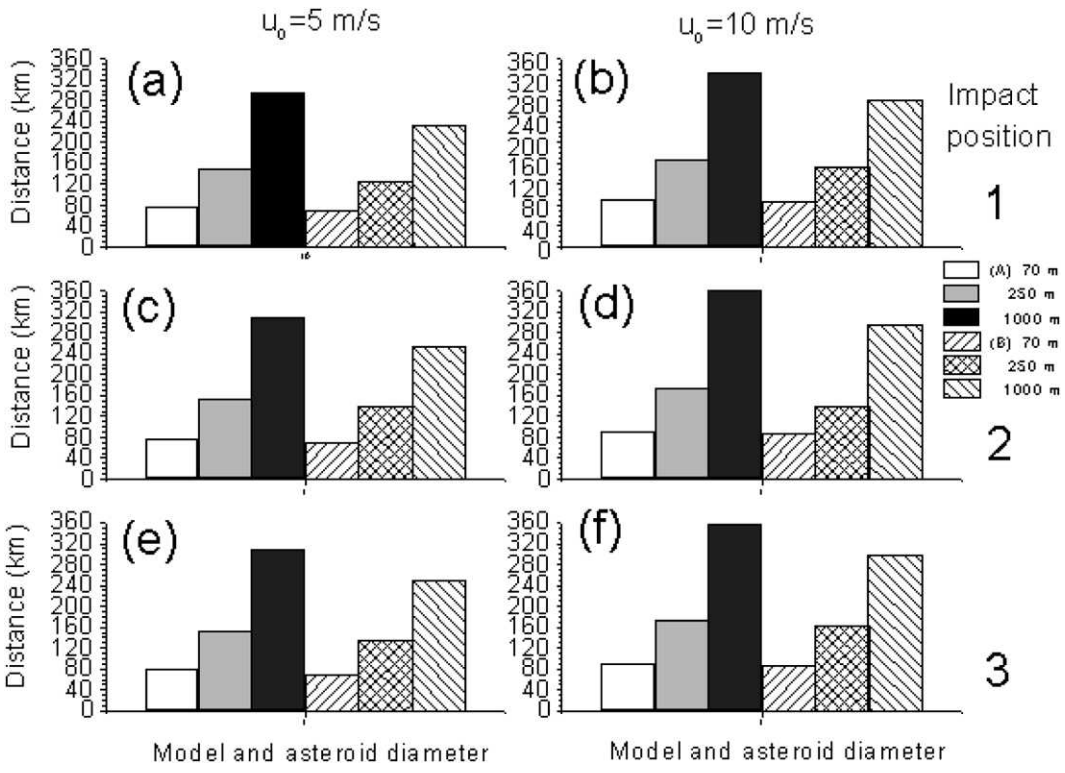

Figure 10. Same as in Figure 9, but for LLC cloud core. LLC denotes the H_2S lower limit concentration.

Under appropriate wind directions, all the large localities on the western Black Sea shore may be affected, whatever the impact position is. The run-in of the LLC cloud core may range between 140 and about 300 km, depending on impact position, wind speed, and direction. Computations show that the size of the LLC cloud core is about 32 km perpendicular to wind direction. The land surface area covered by the LLC cloud core during the run-in ranges between about 4480 and 9600 km^2. This may affect between 107 000 and 230 000 people (apart from the population of the large towns on the seashore). In this evaluation we adopted a population density of 24 people per square kilometer. Note that regions with densities up to 249 people per square kilometer exist near the coast (see Figure 2). Thus, our evaluations may be a few times underestimated for some particular wind directions.

When 250-m-diameter asteroids are considered, the distances traveled by the LLC cloud core range between about 120 and 160 km (depending on model) at a wind speed of 5 m s^{-1} and between about 150 and 180 km (depending on model) at a wind speed of 10 m s^{-1}. Again, these values may be compared with distances in Table 3. All four localities may be affected by the LLC cloud core in case of impacts at position 1. An exception may be Burgas, at the lower wind speed. Impacts at position 2 may affect Mangalia, whatever the wind speed is. The other localities may be affected too under larger wind speed. Impacts at position 3 do not affect Burgas but may affect the other three localities if the wind speed is of the order of 10 m s^{-1}. An exception is Mangalia, which may be affected even for smaller wind speeds. The run-in of LLC cloud core generated at impact position 1 may range between about 20 and 100 km, depending on wind speed and direction. Computations show that the size of the LLC cloud core is about 14 km perpendicular to wind direction. The land surface area covered by the LLC cloud core during the run-in ranges between about 280 and 1400 km^2. For a population density of 24 people per square kilometer, this may affect between about 6000 and 33 000 people (apart from the population of the large towns on the seashore). Our evaluations may be a few times underestimated for some particular wind directions (see discussion above).

In the case of 70-m-diameter asteroids, the distances traveled by the LLC cloud core range between about 70 and 80 km (depending on model) at a wind speed of 5 m s^{-1} and between about 80 and 90 km (depending on model) at a wind speed of 10 m s^{-1}. Comparing these values with distances listed in Table 3 shows that impacts at position 1 may affect Mangalia, whatever the wind speed is. Impacts at positions 2 and 3 do not affect the four major localities on the western Black Sea shore. The run-in of the LLC cloud core generated at impact position 1 may range between about 10 and 30 km, depending on wind speed and direction. Computations show that the size of the LLC cloud core is about 7 km perpendicular to wind direction. The land surface area covered by the LLC cloud core during the run-in ranges between about 70 and 210 km^2. For a population density of 24 people per square kilometer this may affect between about 1600 and 5100 people (apart from the population of the large towns on the seashore). Again, our evaluations may be a few times underestimated for some particular wind directions (see discussion above).

The hazard plays an important role in all phenomena where atmospheric factors are involved. For instance, the dispersion of the poisonous gas cloud is influenced

by the atmospheric turbulence. All the results reported in this paper refer to the Pasquill stability class F. Simulations for different Pasquill classes (A–D) were also performed, keeping the same asteroid size and impact location. The results obtained are different, as expected, with a tendency to decrease the surface area affected by the poisonous cloud when the atmospheric stability class moves from F to A. For instance, in the case of a 70-m-sized impactor, changing the stability class from F to D reduces the distance traveled by the ULC cloud by about 18%, whatever the wind speed is. However, the simulation results keep the main features already emphasized.

Note that the dry land topography was not taken into account when modeling the dispersion process during the run-in. It may have important local effects.

9. Risks for other effects associated with asteroid impacts

The usual effect associated with large asteroids impacting land areas is the generation of severe atmospheric shock waves. When the place impacted is the sea, an additional effect is tsunami generation. Information about the magnitude of these effects is briefly reviewed here. This will give a broader perspective for our findings.

The rule of thumb (derived from nuclear explosion experiments and simulations) is that the impact cavity diameter d_c is about 20 times the asteroid diameter (Paine 1999). Consequently, d_c ranges between about 1 km for a 50-m asteroid and 20 km for a 1-km impactor. The result is that the margins of the impact cavities studied here are relatively far from the seashore, whatever the impactor size is (see Figure 4 for the impact positions and Table 3). Table 1 in Paine (Paine 1999) gives the surface area directly devastated by shock waves generated by asteroids of various sizes. The results there are based on an empirical formula derived by Steel et al. (Steel et al. 1995) from nuclear weapon tests and models. The radius of the devastated area is 24, 48, 96, and 485 km for asteroids with diameters of 50 m, 100 m, 200 m, and 1 km, respectively. The result for the 50-m asteroid is in good agreement with observations about the airburst Tunguska event. Note, however, that for a given energy an airburst has a larger radius of destruction than a ground impact. We may compare the radius of the devastated area with the distances from the impact positions considered here to the coast (see Table 3). The shock waves generated by asteroids less than 100 m in size will not affect the land, whatever their impact position is. Impactors with a diameter of 200 m will not affect the land in the cases of impact positions 2 and 3. For the impact positions 0 and 1, the shock waves will affect Mangalia (and to a lesser extent Varna). The 1-km-sized impactor will devastate large land regions on both the Bulgarian and Romanian coasts.

A brief estimation of the tsunami effects follows. Table 3 of Paine (Paine 1999) shows the estimated deep-water wave height H (above sea level) at a point 100 km away from the asteroid impact location. This quantity is 0.12, 0.7, 3, and 70 m for asteroids of diameters 50 m, 100 m, 200 m, and 1 km, respectively. The run-up factor is defined as the ratio $f_{\text{run-up}} = J/H$, where J is the run-up height. The run-up factor can vary considerably, depending on local shore topography and the direction of travel of the wave. The typical run-up factor for coastal locations is only 2 to 3. Table 6 in Paine (Paine 1999) shows the relative risk of coastal location compared to inland location for various values of the tsunami run-up factor. A

value of $f_{\text{run-up}} = 0$ (i.e., an inland asteroid impact) is associated to a relative risk equal to unity. For values of $f_{\text{run-up}} = 5$, 10, 20, and 40 the relative risk is 4, 11, 46, and 74, respectively. Information about the run-up height is missing in the case of tsunamis generated by asteroids impacting the Black Sea. If we adopt a typical value $f_{\text{run-up}} = 3$, then the relative risk of coastal location compared to inland location is about 2.5.

More recent studies focus on the key distinction between familiar earthquake-generated tsunamis and impact tsunamis (Asphaug et al. 2003). The authors of these studies concluded that impact tsunamis are less dangerous than has been assumed by previous studies, mostly because they have shorter wavelengths than seismic tsunamis and therefore can run in only a kilometer or so at most. Furthermore, with even modest warning the loss of human life can be minimized, since it is necessary only to move a few kilometers inland or to an elevation of a few meters to escape the inundation—thus impact tsunamis are primarily a threat to coastal infrastructure, not populations.

10. Risks for H_2S release by nuclear explosions

The impact by asteroids of the size analyzed in this paper may be considered as a remote risk. There are, however, other risks with greater proximity for a poisonous gas cloud to be released. We are referring here to the situation when very large explosions occur in the deep seawater of the Black Sea. This may happen, for example, in cases where nuclear weapons are deliberately used or in cases of accidental nuclear explosions on submarines.

The energy released by nuclear weapons is usually measured in tons of trinitrotoluene (TNT). Nuclear explosive devices with quite different yields have been built during the years. Some older bombs had yields of about 20 Mton TNT (84 000 TJ), but today most nuclear devices have yields of less than 1 Mton TNT (less than 4000 TJ) (*World Book Encyclopedia*, 1999 ed., s.v. "atomic bomb").

We may compare the energy released by a nuclear explosion with the kinetic energy carried on by an asteroid, which is proportional to the third power of its diameter. As a rough approximation we associate to the Tunguska event a 70-m-diameter asteroid and a 10-Mton TNT explosion. If a nuclear explosion (deliberate or accidental) would occur these days, it is likely the energy released would be less than 1 Mton TNT, that is, more than 10 times smaller than the Tunguska explosion. This explosion would correspond to the impact by a 33-m-diameter asteroid. Thus, the results we presented for the 70-m impactor may be seen as the most pessimistic scenario for a "common" nuclear explosion. A very large 50-Mton TNT nuclear explosion is the equivalent of a 120-m asteroid impact. The effects of this explosion would range between those associated with the 70- and 250-m asteroids, respectively, considered here.

The effects of the nuclear accident that occurred on 26 April 1986 at Chernobyl may be compared with those predicted by the present model. The explosion at Chernobyl was chemical, driven by gases and steam generated by the nuclear reactor core runaway, not by nuclear reactions (Rhodes 1993). Based on the official reports, nearly 8 400 000 people in Belarus, Ukraine, and Russia were exposed to the radiation. Agricultural areas covering nearly 52 000 km^2 were contaminated with cesium-137 and strontium-90 (UNOCHA 2004). One can see

that the surface area affected by the Chernobyl accident is much larger than that affected by the poisonous gas cloud released into the atmosphere by a 1-km impact asteroid. However, the direct effects on human population (in lives lost) may be much more important in the case of poisoning due to the asteroid impact.

11. Risks for H_2S release by earthquakes

The frequency of large earthquakes in the basin of the Black Sea is rather well known. Nine strong earthquakes were described in Dotsenko (Dotsenko 1995), starting from the first century B.C. until 1966. More recently, 22 events were documented for the same time period by comparison of the historical, instrumental, and numerical data (Yalçiner et al. 2004). A comparison between the potential of releasing H_2S by strong earthquakes and by impacts by asteroids, respectively, may be performed indirectly by using information referring to the associated tsunamis. On 12 July 1966 a submarine earthquake occurred not far from Anapa, Russia, accompanied by a tsunami. The epicenter was located approximately 10 km away from the shore at a location with coordinates 44.7°N, 37.2°E. Its focal depth was 55 km, and approximate magnitude and intensity were 5.8 and 6, respectively. Tsunami height was recorded by the tide gauge with a height of 42 cm in Gelendzhik, Russia (50 km south), and 10 cm in Feodosia, Ukraine (60 km across in the Crimean Peninsula). The tsunami generated by the impact of a 70-m asteroid was simulated to have a height of 65 m at a 40-km distance from the impact location (Schuiling et al. 2007). Thus, even if the frequency of strong earthquakes is relatively large, the risk for releasing amounts of H_2S comparable with those generated through impacts by asteroids of the size analyzed in this paper seems to be negligible.

12. Conclusions

The hydrogen sulfide–rich waters of the Black Sea pose a potential danger for the surrounding land regions. The impact of an asteroid exceeding tens of meters in size may cause both a tsunami wave and a catastrophic poisonous gas release in the atmosphere. Some effects of this last phenomenon on the western coastal regions were evaluated.

In the beltlike sea region of variable width with waters less than 200 m in depth, no hydrogen sulfide cloud is generated at impact, due to the small or even null content of dissolved hydrogen sulfide. At the other impact positions, the initial diameter of the hydrogen sulfide cloud depends on asteroid size. It is about 2580, 4916, and 12288 m, for $D_i = 70$, 250, and 1000 m, respectively, whatever the impact location is. The initial thickness of the poisonous cloud depends, in addition, on sea depth at impact location and on the model adopted for cloud formation.

Two hydrogen sulfide concentrations in the cloud are of particular interest: the lower concentration limit (LLC) of 19.88 ppm (associated with fatigue, loss of appetite, headache, irritability, poor memory, and dizziness) and the upper concentration limit (ULC) of 497 ppm (associated to death after single exposure).

Three asteroid impact positions were considered for more detailed study. These locations are about a 40-km distance each other (see Figure 4). The nearest site on the coast is about 60 km from impact position 1.

The wind speed plays an important role in H_2S cloud dynamics. At low wind speeds (0.5 m s^{-1}), for example, the cloud generated by a 250-m-sized asteroid is still almost centered on the impact location for more than a half-day after the impact. This ULC cloud core lasts for more than 33 h and travels on wind directions less than 40 km from the impact location. The LLC cloud core lasts for about three days and travels on wind direction about 75 km. At a higher wind speed value (10 m s^{-1}), the ULC cloud core may travel about 60 km in less than 1 h and 20 min after the impact. This core, with a size of about 4 km × 10 km in its final stages, lasts for about 100 min and travels about 70 km from the impact position. The LLC cloud core travels 150 km in about 2.8 h. Its last stages size may be about 12 km × 12 km.

The maximum distance traveled by the ULC and LLC cloud cores increases by increasing the asteroid size and wind speed. The influence of the impact position on the distance traveled by hydrogen sulfide clouds is rather weak, as long as the seawater depth does not change significantly.

The land surface area covered by the ULC cloud core generated by a 1000-m-sized asteroid during the run-in may be as high as 1920 km^2 (for the inputs used in this paper). This may affect up to 478 000 people. The surface area affected by the poisonous gas cloud is much smaller than the surface area affected by the Chernobyl nuclear accident. However, the effects on human population may be much more important in case of the asteroid impact. In case of a 250-m-diameter asteroid, the population affected by the ULC cloud core may be as large in number as 24 900 people. These estimates do not include the population of the towns on the shore. The ULC cloud cores generated by 70-m-diameter asteroids travel for about 30 km and do not reach the shore, whatever the impact position is.

The land surface area covered by the LLC cloud core generated by a 1000-m-sized asteroid during the run-in ranges between about 4480 and 9600 km^2. This may affect between 107 000 and 230 000 people. When a 250-m-sized asteroid is considered, the land surface area covered by the LLC cloud core during the run-in ranges between about 280 and 1400 km^2. This may affect between about 6000 and 33 000 people. In the case of a 70-m asteroid, the LLC cloud core covers between 70 and 210 km^2 during the run-in. This may affect between about 1600 and 5100 people. These evaluations do not include the population of the towns on the seashore and may be a few times underestimated for some particular wind directions.

Very large explosions may occur in the deep seawater of the Black Sea as a result of deliberate use of nuclear weapons or in case of accidents on submarines. The underwater explosion of a ("common") 1-Mton TNT bomb may be assimilated to the impact by an asteroid with a diameter of 33 m. The effects of a very large 50-Mton TNT explosion would range between those associated to the 70- and 250-m asteroids considered here.

Acknowledgments. The author thanks Prof. R. D. Schuiling (Utrecht University), Prof. E. Pelinovsky (Institute of Applied Physics, Nizhny Novgorod), Dr. D. Isvoranu (Polytechnic University of Bucharest), and Mr. R. B. Cathcart (Geographos, Glendale, California) for stimulating discussions. Also, the useful comments and suggestions by the referees are acknowledged.

REFERENCES

Ahlborg, G., 1951: Hydrogen sulfide poisoning in shale oil industry. *Arch. Ind. Hygiene Occup. Med.,* **3,** 247–266.

Aiuppa, A., A. Franco, R. von Glasow, A. G. Allen, W. D'Alessandro, T. A. Mather, D. M. Pyle, and M. Valenza, 2006: The tropospheric processing of acidic gases and hydrogen sulphide in volcanic gas plumes as inferred from field and model investigations. *Atmos. Chem. Phys. Discuss.,* **6,** 11 653–11 680.

Asphaug, E., D. Korycansky, and S. Ward, 2003: Ocean waves from asteroid impacts. *Eos, Trans. Amer. Geophys. Union,* **84,** 339.

ATSDR, 1999: Toxicological profile for hydrogen sulfide. Department of Health and Human Services, Agency for Toxic Substances and Disease Registry, Atlanta, GA, 253 pp.

Beauchamp, R. O., Jr., J. S. Bus, J. A. Popp, C. J. Boreiko, and D. A. Andjelkovich, 1984: A critical review of the literature on hydrogen sulfide toxicity. *Crit. Rev. Toxicol.,* **13,** 25–97.

Beychok, M. R., 2005: *Fundamentals of Stack Gas Dispersion.* 4th ed. Milton Beychok Publishers, 201 pp.

Bland, P. A., and N. A. Artemieva, 2003: Efficient disruption of small asteroids by Earth's atmosphere. *Nature,* **424,** 288–291.

Chapman C. R., D. D. Durda, and R. E. Gold, 2001: The comet/asteroid impact hazard: A systems approach. SwRI White Paper, 19 pp. [Available from Office of Space Studies, Southwest Research Institute, Boulder, CO 80302 and online at www.boulder.swri.edu/clark/neowp.html.]

Chou, C.-H., 2003: Hydrogen sulfide: Human health aspects. Concise International Chemical Assessment Document 53, World Health Organization, Geneva, Switzerland, 41 pp.

CIESIN, cited 2006: Gridded population of the world: Future estimates (GPWFE). Socioeconomic Data and Applications Center, Columbia University; Center for International Earth Science Information Network, Columbia University; United Nations Food and Agriculture Programme; and Centro Internacional de Agricultura Tropical. [Available online at http://sedac.CIESIN.columbia.edu/gpw.]

Dotsenko, S. F., 1995: The Black Sea tsunamis. *Atmos. Oceanic Phys.,* **30,** 483–489.

Foschini, L., 1999: A solution for the Tunguska event. *Astron. Astrophys.,* **342,** L1–L4.

Gisler, G., R. Weaver, C. Mader, and M. L. Gittings, 2003: Two- and three-dimensional simulations of asteroid ocean impacts. *Sci. Tsunami Hazards,* **21,** 119–134.

Havens, J. A., 1988a: A dispersion model for elevated dense gas jet chemical releases. Vol. I, 63 pp. [Available from U.S. Environmental Protection Agency, Office of Air and Radiation, Office of Air Quality Planning and Standards, Research Triangle Park, NC 27711.]

——, 1988b: A dispersion model for elevated dense gas jet chemical releases. Vol. II, 87 pp. [Available from U.S. Environmental Protection Agency, Office of Air and Radiation, Office of Air Quality Planning and Standards, Research Triangle Park, NC 27711.]

——, and T. O. Spicer, 1985: Development of an atmospheric dispersion model for heavier-than-air gas mixtures. Final Report to U.S. Coast Guard CG-D-23-80, USCG HQ, Washington, DC, 104 pp.

Hill, F. B., 1973: Atmospheric sulfur and its links to the biota. *Brookhaven Symp. Biol.,* **30,** 159–181.

HSDB, 1998: Hazardous substances data bank. National Library of Medicine, National Toxicology Program, Bethesda, MD. [Available online at http://toxnet.nlm.nih.gov.]

Humborg, C., V. Ittekkot, A. Cociasu, and B. Bodungen, 1997: Effect of Danube River dam on Black Sea biogeochemistry and ecosystem structure. *Nature,* **386,** 385–388.

IPCS, 2000: International Chemical Safety Card—Hydrogen sulfide. World Health Organization, International Programme on Chemical Safety (ICSC 0165), Geneva, Switzerland. [Available online at http://www.ilo.org/public/english/protection/safework/cis/products/icsc/dtasht/_icsc01/icsc0165.htm.]

Ivezic, Z., and Coauthors, 2001: Solar system objects observed in the Sloan Digital Sky Survey commissioning data. *Astron. J.,* **122,** 2749–2784.

Jewitt, D., 2000: Eyes wide shut. *Nature,* **403,** 145–146.

Kharif, C., and E. Pelinovsky, 2005: Asteroid impact tsunamis. *C. R. Phys.,* **6,** 361–366.

Neretin, L. N., and I. I. Volkov, 1995: On the vertical distribution of hydrogen sulfide in deep waters of the Black Sea. *Oceanology,* **35,** 60–65. (Translated from Russion.)

——, and ——, 1999: Hydrogen sulfide production in the Black Sea: A calculation based on the increment of total inorganic carbon. *Doklady Earth Sci.,* **365A,** 398–401.

Paine, M. P., 1999: Asteroid impacts: The extra hazard due to tsunami. *Sci. Tsunami Hazards,* **17,** 155–166.

Rhodes, R., 1993: *Nuclear Renewal.* Penguin Books, 127 pp.

Schuiling, R. D., R. B. Cathcart, and V. Badescu, 2007: Asteroid impact in the Black Sea: A black scenario. *Soft Matter under Exogenic Impacts,* S. J. Rzoska and V. A. Mazur, Eds., NATO Science Series II: Mathematics, Physics, and Chemistry, Vol. 242, Springer, 1–8.

——, ——, ——, D. Isvoranu, and E. Pelynovski, 2007: Asteroid in the Black Sea: Death by drowning or by asphyxiation? *Nat. Hazards,* **40,** 327–338.

Smith, W. H. F., and D. T. Sandwell, 1997: Global sea floor topography from satellite altimetry and ship depth soundings. *Science,* **277,** 1956–1962.

Spicer, T. O., and J. Havens, 1992: User's guide for the DEGADIS 2.1 Dense Gas Dispersion Model. EPA-450/4-89-019, National Technical Information Service, Document No. PB90-213893, 104 pp. [Available from National Technical Information Service, 5285 Port Royal Rd, Springfield, VA 22161.]

Steel, D., D. Asher, W. Napier, and S. Clube, 1995: *Are Impacts Correlated in Time? Hazards Due to Comets and Asteroids.* University of Arizona Press, 463 pp.

Thompson, R. C., 1976: Behavior of hydrogen sulfide in the atmosphere and its effects on vegetation. NSF Rep. NSF/RA760398, NTIS Publication No. PB-262733, Report to the National Science Foundation, Research Applied to National Needs, Washington, DC, 199 pp.

Toon, O. B., K. Zahnle, D. Morrison, R. P. Turco, and C. Covey, 1997: Environmental perturbations caused by the impacts of asteroids and comets. *Rev. Geophys.,* **35,** 41–78.

UNOCHA, 2004: The United Nations Chernobyl Forum, Vienna 10–11 March 2004. [Available online at http://www-ns.iaea.org/meetings/rw-summaries/chernobyl_forum.htm.]

Ward, S. N., and E. Asphaug, 2000: Asteroid impact tsunami: A probabilistic hazard assessment. *Icarus,* **145,** 64–78.

WHO, 1993: Guidelines for drinking-water quality. 2d ed. Health Criteria and Other Supporting Information, Vol. 2, World Health Organization, Geneva, Switzerland, 48 pp.

Yalçiner, A., E. Pelinovsky, T. Talipova, A. Kurkin, A. Kozelkov, and A. Zaitsev, 2004: Tsunamis in the Black Sea: Comparison of the historical, instrumental, and numerical data. *J. Geophys. Res.,* **109,** C12023, doi:10.1029/2003JC002113.